ORIGINAL RESEARCH (AR)

DOI: 10.4274/jems.2026.01346

Journal of ETA Maritime Science

Techno-Economic and Environmental Assessment of an ORC-Based Waste Heat Recovery and Cold Ironing System for an Offshore Platform Supply Vessel

Ceren Çelebi[1], Olgun Konur[1], Süleyman Aykut Korkmaz[2]

[1]Dokuz Eylül University Faculty of Maritime, Department of Marine Engineering, İzmir, Türkiye
[2]University of Southampton Faculty of Engineering, Boldrewood Innovation Campus, Department of Civil, Maritime and Environmental Engineering, Southampton, United Kingdom

Abstract

The maritime industry is under increasing pressure to comply with International Maritime Organization (IMO) regulations targeting net-zero greenhouse gas emissions by 2050. This study evaluates an Organic Rankine Cycle (ORC)-based waste heat recovery system integrated into an offshore platform supply vessel, explicitly considering four distinct operating modes: cruising, dynamic positioning, standby, and port. A steady-state thermodynamic ORC model developed in MATLAB is employed to represent average operating conditions in each mode. Among the ten candidate working fluids, R1233zd(E) is identified as optimal, delivering a net power output of 192.74 kW at full engine load. Four energy management scenarios are examined: a conventional baseline, integration of an ORC, an ORC-battery hybrid system, and an ORC system combined with cold ironing during port operations. The results indicate that the ORC-cold ironing configuration achieves the highest environmental benefit, reducing total cycle-level $CO_{2\text{-eq}}$ emissions by approximately 26.7% relative to the baseline case. From an economic perspective, direct ORC integration yields the lowest levelized cost of energy of $0.1481/kWh and a discounted payback period of 6.27 years, while the ORC-cold ironing configuration has a payback period of 7.70 years. Sensitivity analysis demonstrates that fuel price escalation and carbon taxation are the dominant drivers affecting economic feasibility.

Keywords: Organic rankine cycle, waste heat recovery, cold ironing, techno-economic analysis, platform supply vessel

1. Introduction

The global maritime industry, the backbone of international trade, stands at a critical juncture amid the climate crisis and stringent regulations. The International Maritime Organization (IMO) aims to cut carbon intensity in shipping by at least 40% by 2030 and 70% by 2040 compared to 2008 levels, striving for net-zero greenhouse gas emissions by around 2050 [1]. This vision is being implemented through mandatory measures such as the Energy Efficiency Existing Ship Index (EEXI) and the Carbon Intensity Indicator (CII), which rate ship efficiency and require improvements for underperforming vessels [2,3]. Additionally, regional policies, such as the European Union's (EU) Emissions Trading System and the FuelEU Maritime Regulation, increase pressure on shipowners to reduce emissions and adopt low-carbon technologies. The IMO's latest adoption by the Marine Environment Protection Committee (MEPC 83) [4] establishes a carbon-pricing mechanism for the shipping industry and encourages companies to reduce emissions to avoid additional costs. This has spurred research into and development of decarbonization solutions, focusing on eliminating emissions and enhancing energy efficiency to reduce fuel consumption during ship and port operations. This imperative for enhanced maritime operations has given rise to two principal streams of research and technological development: solutions to eliminate emissions, and technologies to improve energy efficiency and reduce fuel consumption in ship and port operations. The IMO lists some key methods to be applied to ships under

Address for Correspondence: Ceren Çelebi, Dokuz Eylül University Faculty of Maritime, Department of Marine Engineering, İzmir, Türkiye
E-mail: crncelebi@hotmail.com
ORCID iD: orcid.org/0009-0007-8505-0419

Received: 15.02.2026
Last Revision Received: 18.05.2026
Accepted: 28.05.2026
Epub: 16.06.2026

To cite this article: C. Çelebi, O. Konur, and S. A. Korkmaz. "Techno-economic and environmental assessment of an ORC-based waste heat recovery and cold ironing system for an offshore platform supply vessel," *Journal of ETA Maritime Science*, [Epub Ahead of Print]

Copyright© 2026 the Author(s). Published by Galenos Publishing House on behalf of UCTEA Chamber of Marine Engineers.
This is an open access article under the Creative Commons Attribution-NonCommercial 4.0 International (CC BY-NC 4.0) License.

draft copy

the Ship Energy Efficiency Management Plan guidelines [5]. Ship operators have historically prioritized readily accessible, low-complexity operational measures; however, recent regulations require greater consideration of their implementation. Among them, cold ironing and Organic Rankine Cycle (ORC) technologies, which have great potential to reduce ship-based emissions, have attracted significant attention despite their relatively high investment costs. Both measures can be considered favorable because of their retrofitting potential, high emission-reduction capacity, technological maturity, and availability of best practices in ship energy systems [6,7].

1.1. Cold Ironing: Environmental, Economic and Infrastructural Perspectives

Research on cold ironing consistently highlights that at-berth (hoteling) emissions are the dominant contributor to overall port-area pollution. Empirical analyses show that hoteling alone can account for more than 70% of total ship emissions for vessels with average port stays, increasing to over 90% for extended stays, underscoring the importance of targeting port operations [8]. Large-scale assessments further demonstrate the mitigation potential of cold ironing, with projected reductions of 96-97% in local pollutants (NO_x and SO_x) and up to 53% in CO_2 emissions across major European ports [9]. However, these studies also emphasize that the net climate benefit of cold ironing is strongly dependent on the carbon intensity of the electricity supplied.

Beyond the environmental and public health benefits, several studies have examined the economic and socioeconomic justification for cold ironing investments. Canepa et al. [10] quantified the societal benefits of shore power by translating reduced gaseous emissions into avoided public health costs, reporting annual savings of approximately €2.27 million for the Port of Genoa. From an operator-oriented perspective, Qiu et al. [11] proposed a tri-level pricing framework that integrates carbon emissions into time-of-use electricity pricing, demonstrating reduced grid congestion, lower emissions, and improved service-provider profitability. The economic relevance of cold ironing within regulatory compliance pathways has also been highlighted, for instance, by Gianni et al. [12], who evaluated shoreside power alongside alternative solutions such as Liquefied Natural Gas (LNG) and Solid Oxide Fuel Cells (SOFCs).

Despite these demonstrated benefits, large-scale implementation remains constrained by practical barriers. Empirical studies identify high initial investment costs, limited electrical infrastructure, and the lack of technical standardization as key obstacles. For example, Le [13] showed that these factors represent the primary barriers in developing regions, while Glavinović et al. [14] reported that approximately 60% of Croatian ports lack the minimum required electrical power capacity, underscoring the need for coordinated infrastructure development and regulatory support.

Recent studies demonstrate that the emission reduction effectiveness of cold ironing is strongly dependent on the carbon intensity of the supplied electricity; when fossil-based grid power is considered, the overall mitigation potential is significantly reduced [15]. To address this limitation, renewable-integrated cold ironing configurations combining photovoltaics (PV) and energy storage have been shown to substantially improve both environmental and economic performance, achieving up to a 63.4% reduction in operational costs in ferry applications [16]. More advanced hybrid systems incorporating PV, batteries, and hydrogen-based energy carriers can nearly eliminate $CO_{2\text{-eq}}$ emissions; however, green ammonia-based solutions remain economically challenging, rendering grid-powered and PV-battery configurations more viable in the near term [17]. While cold ironing primarily targets port-related emissions, complementary ship-side solutions, such as hybrid diesel-battery systems with waste heat charging, have also been proposed to enhance at-sea efficiency [18].

1.2. ORC Systems in Maritime Applications

ORC technology has emerged as a leading waste heat recovery (WHR) solution for enhancing maritime energy efficiency. Literature reviews indicate that standard marine ORC systems typically exhibit conversion efficiencies below 20%, but fuel savings of 3-5% are achievable depending on the system configuration and operational profile [6,19]. These benefits can be further amplified through advanced integration strategies, such as combined-cycle arrangements or the utilization of LNG cold energy [6]. Beyond theoretical assessments, research has increasingly focused on ORC performance under practical marine constraints. Component-level optimization, specifically regarding expander and turbine design, is critical for maximizing fuel consumption reductions [20]. Furthermore, working fluid selection remains a pivotal factor; comparative studies emphasize that fluid thermophysical properties must be carefully matched to heat-source temperatures to minimize thermodynamic irreversibilities [21,22]. Finally, voyage-based analyses reveal that ORC efficacy is highly sensitive to engine load and ambient conditions, underscoring the necessity of accounting for operational variability in long-term performance estimations [23,24].

Recent literature increasingly explores ORC integration within hybrid ship energy systems to enhance overall system performance. These concepts include cogeneration, alternative fuel-based power systems, and carbon capture applications, where ORCs act as bottoming cycles in multi-stage WHR layouts [25-27]. Such integrated configurations

Draft Copy

have reported overall efficiencies exceeding 60% when coupled with technologies such as SOFCs operating on methanol or ammonia [26,27]. Similarly, ORC-assisted hybrid systems proposed for LNG carriers support boil-off gas re-liquefaction and carbon capture, achieving payback periods (PBP) as low as 1.55-3.78 years [28,29]. Additional integrations with supercritical CO_2 cycles or wind-assisted propulsion further indicate a broader transition toward highly integrated ship energy systems employing ORCs as bottoming cycles [30,31].

Despite the significant technical potential of ORC systems, their economic viability remains a central challenge. Recognizing that high capital costs and limited operating hours can lead to long PBPs, researchers have focused on innovative strategies to improve the economic case. Kosmadakis and Neofytou [32], proposed a novel reversible unit that functions as an ORC at sea and a high-temperature heat pump in port, thereby maximizing the equipment's annual operational hours and achieving an attractive PBP of 3.5 to 5 years. In a similar effort to extend operational time, Konur et al. [33], designed an innovative ORC system for a large tanker that utilizes waste heat from both the main engine during navigation and the cargo oil pump turbines during port operations, improving the PBP to 6.2 years. Identifying and exploiting all available heat sources across different operational modes is crucial.

1.3. Research Gap, Novelty and Contribution

The literature review above highlights a clear dichotomy in maritime decarbonization research: cold ironing is predominantly investigated as a static, at-berth emission-mitigation measure, whereas ORC systems are primarily assessed as dynamic solutions for improving at-sea energy efficiency. Although recent ORC studies have begun to account for operational variability [33], the literature remains largely focused on conventional vessel types, such as tankers and container ships, characterized by relatively predictable navigation and port operation profiles. As a result, vessels with complex and highly variable duty cycles, particularly offshore platform supply vessels (PSVs), remain underexplored. In contrast to conventional ships, PSVs operate across four energetically distinct modes: high-power dynamic positioning (DP), cruising, low-power standby, and port hoteling. For such vessels, the economic viability of an ORC system is governed by its cumulative annual energy recovery, which depends on the substantial variations in waste heat availability and quality across these modes. Addressing this gap, the present study provides a comparative techno-economic and environmental assessment of the base case and of an ORC system integrated into three energy-management scenarios: (i) ORC integration into the base case only, (ii) ORC-battery hybrid system configuration, and (iii) an ORC system combined with cold ironing during port operations. The novelty lies in analyzing the ORC technology and its battery-hybrid configuration across the vessel's varying operational profile and in providing the vessel's energy demand during cold ironing at port, thereby capturing emission-reduction potentials across cruising, DP, standby, and port-hoteling operating conditions, and assessing the economic feasibility of these scenarios. The results offer valuable insights for shipowners and designers seeking viable pathways to meet increasingly stringent efficiency and emissions regulations in the maritime sector.

2. Methodology

This study focuses on the design and evaluation of an ORC-based WHR system integrated into an offshore PSV. A vessel and its main diesel generator were selected as the basis for the analysis.

2.1. Vessel and Generator Specifications

The study considers a PSV with an overall length of 73.6 m, a beam of 16 m, a gross tonnage of 2,180, and a summer deadweight tonnage of 3,326 t. The vessel was built in Aukra, Norway, in 2009. Propulsion is provided by a MAN 5S35ME-C9.7 HL main engine rated at 3,980 kW and operating at 167 rpm. Electrical power is supplied by a Nogva Scania DI 12 62M generator with a rated capacity of 310 kVA at 1,800 rpm.

The fuel consumption characteristics of the selected generator are summarized in Table 1 [34]. The specific fuel consumption (SFC) values for different load conditions serve as the basis for the load-dependent fuel consumption model used in this study.

Table 1. *Consumption data of the existing generator in the selected vessel [34]*

Engine performance parameters for different load conditions	1500 RPM	1800 RPM
Gross power (kW)	280	285
Specific fuel consumption (g/kWh) at Full Load	206	209
Specific fuel consumption (g/kWh) at 3/4 Load	208	207
Specific fuel consumption (g/kWh) at 1/2 load	208	212

These data are used to estimate the generator's fuel consumption under different vessel operating modes. The total fuel consumption of the generator, in kg, is calculated using Equation 1.

$$m_{fuel} = SFC \times P \times t \quad (1)$$

draft copy

where m_{fuel} is the total fuel consumption (kg), SFC is the SFC (kg/kWh), P is the generator power (kW), and t is the operation time (h).

2.2. ORC Unit

This study evaluates an ORC-based WHR system designed to capture waste heat from the main engine of an offshore PSV and thereby reduce fuel consumption. The system comprises a boiler plant that captures heat from the exhaust gases and an ORC plant that converts this thermal energy into electrical power. The exhaust gas temperature and flow rate as functions of the main engine load are shown in Figure 1.

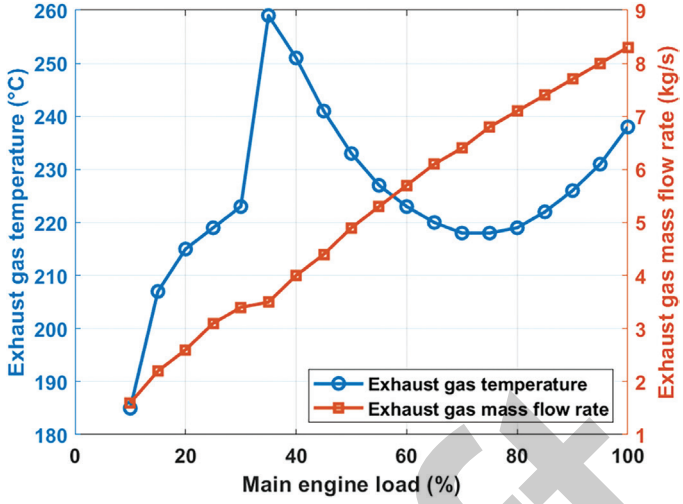

Figure 1. *Main engine exhaust gas parameters [35]*

The ORC system is modeled as a steady-state thermodynamic cycle consisting of an evaporator, turbine, condenser, and pump. Thermophysical properties of the working fluids are obtained using the CoolProp library integrated into MATLAB. The condenser outlet temperature is fixed at 40 °C. The available exhaust gas heat rate ($\dot{Q}_{exh}$) is calculated according to Equation 2.

$$\dot{Q}_{exh} = \dot{m}_{exh(i)} \times c_p \times (T_{in(i)} - T_{out}) \quad (2)$$

where $\dot{m}_{exh}$ and T_{in} are the exhaust gas mass flow rate and inlet temperature corresponding to the operating mode i, which are given in Figure 1. c_p is the exhaust gas specific heat capacity (1,089 J $kg^{-1}K^{-1}$), and T_{out} is the exhaust gas outlet temperature, fixed at 80 °C. The heat input to the ORC evaporator is determined from the exhaust heat rate and the assumed heat exchanger efficiency of 99%. The working fluid mass flow rate ($\dot{m}_{wf}$) is obtained from the evaporator energy balance, using Equation 3.

$$\dot{Q}_{evap} = \dot{m}_{wf} \times (h_1 - h_4) \quad (3)$$

Here, $\dot{Q}_{evap}$ is the heat input to the ORC evaporator, which is calculated using $\dot{Q}_{exh}$ and heat exchanger efficiency (η_{HEX}), where h_1 and h_4 represent the specific enthalpies at the evaporator outlet and pump outlet, respectively. The evaporator outlet enthalpy h_1 is evaluated assuming a 7 K superheated vapor state at the evaporator pressure. The value of h_4 is derived using the pump isentropic efficiency equation, as shown in Equation 4.

$$h_4 = h_3 + \frac{v_f \times \Delta P}{\eta_p} \quad (4)$$

Where η_p is the pump isentropic efficiency, h_3 and v_f are the specific enthalpy and specific volume at the condenser outlet, evaluated under saturated liquid conditions. The pressure difference (in Pa) is calculated as the difference between the ORC evaporator and condenser pressures. The net electrical power output of the ORC system is $\dot{W}_{net}$) calculated using Equation 5 in Watts.

$$\dot{W}_{net} = \dot{m}_{wf} \times [(h_1 - h_2) - (h_4 - h_3)] \quad (5)$$

The turbine outlet enthalpy, h_2, is determined using an 80% isentropic efficiency, η_t as shown in Equation 6. The pump and turbine isentropic efficiencies were assumed as 80% based on literature values [24].

$$h_2 = h_1 - \eta_t \times (h_1 - h_{2s}) \quad (6)$$

The isentropic turbine outlet enthalpy, h_{2s}, is determined at the condenser pressure using the entropy at the turbine inlet. The calculation is performed using the evaporator outlet pressure and temperature.

Finally, Equation 7 is used to calculate the net electrical energy recovered from the ORC system, E_{net}, (in units of Wh), considering the operating duration. These results were then converted into kWh.

$$E_{net} = \dot{W}_{net} \times t(i) \quad (7)$$

2.3. Working Fluid Selection

The performance and environmental footprint of an ORC system are strongly governed by working fluid properties, particularly ozone depletion potential, global warming potential (GWP), and the degree of superheating, which directly affects cycle efficiency [6].

For the designed ORC-integrated WHR system, 10 candidate working fluids were selected from the literature on marine ORC systems [6,23,36-38]. Table 2 provides detailed information on the properties of these candidate working fluids.

draft copy

Table 2. *Properties of the organic working fluids [23,39,40]*

Organic working fluid	GWP	ODP	ASHRAE 34	Critical temperature (°C)	Critical pressure (kPa)
R245fa	962	0	A1	154	3,651
R1233zd(E)	3.88	0	A1	165.6	3,573
R1234yf	4	0	A2L	94.7	3,382
R134a	1,430	0	A1	101	4,059
R152a	124	0	A2	113.3	4,520
R227ea	3,500	0	-	102.8	2,980
R236fa	9,400	0	A1	124.9	3,200
R600	0.006	0	A3	152	3,796
R1234ze(Z)	0.88	0	A2L	150.1	3,533
R236ea	1,500	0	A1	139.3	3,429
ODP: Ozone depletion potential, GWP: Global warming potential					

The ORC performance when using various fluids (Table 2) is evaluated under different vessel operating modes using load-dependent exhaust gas temperature and mass flow rate data. The corresponding net power output and recovered electrical energy are calculated for each operating mode.

2.4. Operating Modes and Case Definitions

The base case excludes the ORC system and relies entirely on fuel-based generators, whereas all other cases incorporate the ORC system. The ORC power output is evaluated for each operating mode using the load conditions given in Table 3. The table summarizes the vessel's operational profile across different operating modes, including engine load, exhaust gas conditions, power demand, and duration of each mode for one duty cycle of the PSV. Two separate cruising phases, Cruise 1 and Cruise 2, are defined to represent outbound and return voyages, respectively.

The performance of the proposed ORC-based WHR system was evaluated through various case studies, each defined by a different energy management strategy. In the base case, no WHR system is installed, and all onboard electrical demand is supplied solely by diesel generators.

In Case 1, an ORC-based WHR system is integrated, and the electrical power generated by the ORC is directly supplied to the vessel's electrical load, thereby reducing the generator load. During port operations, electrical demand is met by generators.

In Case 2, the ORC system is coupled with a battery energy storage system. The electrical power generated by the ORC is primarily used to charge the batteries, which are subsequently discharged during port operations to fully supply the vessel's electrical demand. When the battery system is fully charged, the excess ORC power is directly supplied to the vessel. The battery capacity is sized to ensure an uninterrupted power supply throughout port operations.

In Case 3, the ORC system operates identically to Case 1 during navigation and standby modes; however, during port operations, the onboard electrical demand is supplied by cold ironing instead of generators. Shore power is assumed to be provided by either the national electrical grid-mix or the grid-PV sources through renewable energy contracts, thereby eliminating fuel consumption and direct emissions during port stays.

A schematic representation of each case is given in Figure 2.

In all cases, the electrical power balance is evaluated mode by mode. The required generator power is determined by subtracting the power supplied by the ORC system and/or battery storage, depending on the selected configuration. The number of operating generators is then identified based

Table 3. *Parameters for each operation mode*

Parameter	Cruise 1	DP	Standby	Cruise 2	Port
Load (%)	85	85	60	85	-
Main engine exhaust gas temperature (°C)	222	222	223	222	-
Exhaust gas mass flow rate (kg/s)	7.4	7.4	5.7	7.4	-
Duration (h)	8	16	184	8	72
Power demand (kW)	600	600	600	600	150

draft copy

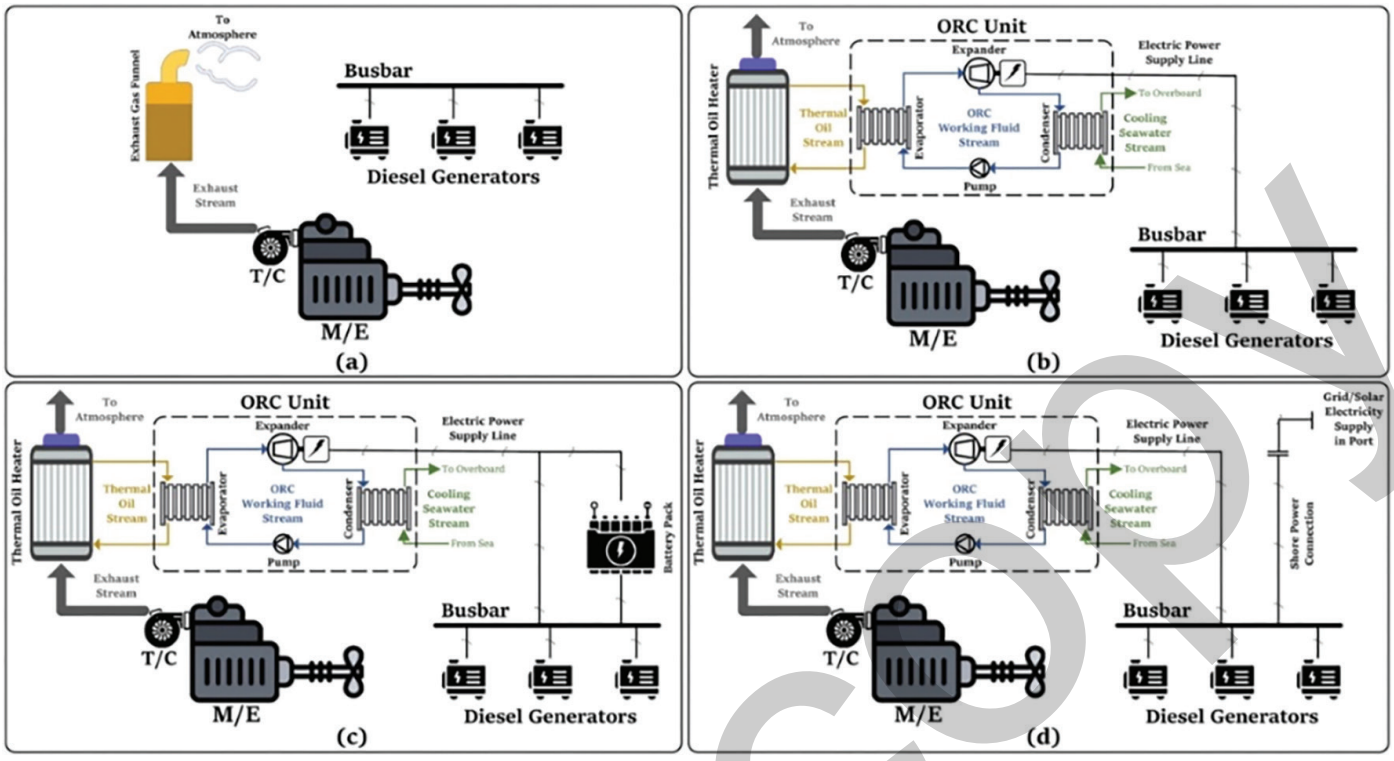

Figure 2. *Power supply system configurations of offshore PSV for* ***(a)*** *Base case* ***(b)*** *Case 1-ORC integrated configuration* ***(c)*** *Case 2-ORC and battery hybrid configuration* ***(d)*** *Case 3-ORC and cold ironing in port with grid-PV electricity/ORC and cold ironing in port with grid-mix electricity*

on the remaining power demand and the rated capacity of a single generator (285 kW). Subsequently, the power output per generator is calculated, and the corresponding load fraction is obtained using Equation 8.

$$load\,(\%) = \frac{P_{gen}}{P_{gen,max}} \times 100 \quad (8)$$

Where P_{gen} is the actual electrical output per operating generator (kW), determined from the vessel's power demand after accounting for ORC contribution and the number of active generators, and $P_{gen,max}$ is the rated maximum capacity of a single generator (kW).

SFC is determined through interpolation based on the calculated load. The energy supplied by generators, denoted E_{gen} (kWh), is calculated based on the duration of each port's operational mode. Subsequently, fuel consumption (kg) for each mode is derived using Equation 9.

$$m_{fuel,\,(i)} = SFC \times E_{gen} \quad (9)$$

The total fuel consumption is calculated by summing the fuel consumption (kg) of each mode. The vessel consumes only MGO for the main engine and the generators' fuel requirements during all operations. Figure 3 presents the logic schematic used to determine the number of operating generators, their load distribution, and the corresponding fuel consumption for the defined case studies.

Cases 1 and 3 employ an identical calculation procedure, except in port operations: Case 1 relies on generators (MGO), whereas Case 3 uses cold ironing. For Case 2, the power supply is governed by the battery. The battery system is sized at 10,951 kWh (47 modules × 233 kWh) to ensure 72 hours of uninterrupted 150 kW port power (10,800 kWh total requirement).

2.5 Environmental Impacts

Subsequently, the environmental impacts are evaluated for each case. Carbon dioxide equivalent ($CO_{2\text{-eq}}$) emissions are calculated using MGO fuel emission conversion factors, expressed as grams of $CO_{2\text{-eq}}$ per gram of fuel completely combusted, together with 100-year GWPs [41]. The corresponding emission factors and GWP values adopted in this study are summarized in Table 4.

The calculation is performed using Equation 10 [41]. The adopted emission conversion factors and GWP values are provided in Table 4.

$$EF_{MGO} = \sum(Cf_p \times GWP_p) \quad (10)$$

draft copy

Table 4. *MGO Fuel carbon dioxide equivalent emission conversion factors (g CO_2/g fuel completely combusted) and GWP over 100-year values [41,42]*

Fuel	Cf_{CO_2}	Cf_{CH_4}	Cf_{N_2O}	GWP_{CO_2}	GWP_{CH_4}	GWP_{N_2O}
MGO	3.206	0.00005	0.00018	1	28	265

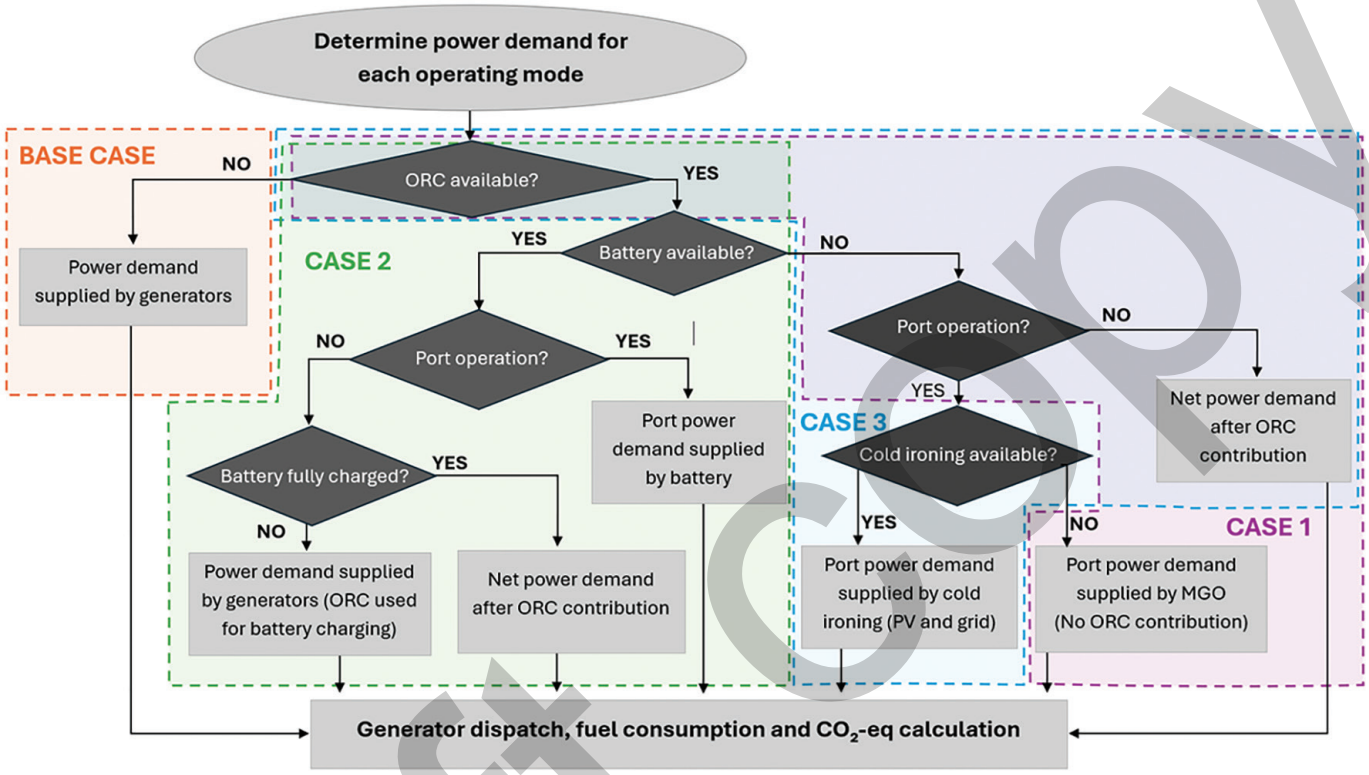

Figure 3. *Decision logic for generator dispatch and power supply under the defined operating modes and case studies*

Where EF_{MGO} is the total $CO_{2\text{-eq}}$ emission factor of MGO fuel (kg $CO_{2\text{-eq}}$ /kg fuel), $C_{f,p}$ is the emission conversion factor of the pollutant p (g/g fuel), and GWP_p is the corresponding 100-year GWP. This is followed by $CO_{2\text{-eq}}$ for total fuel consumption per case, calculated by multiplying total fuel consumption (kg) by EF_{MGO}.

For Grid and PV, $CO_{2\text{-eq}}$ per energy values are reported in kg/kWh, with values of 0.478 and 0.033, respectively [43], [44]. The $CO_{2\text{-eq}}$ (kg) for total fuel consumption per case is calculated by multiplying the port energy demand (kWh) by the $CO_{2\text{-eq}}$ per energy unit (kg/kWh).

2.6. Economic Analysis

An economic assessment is conducted to evaluate the cost implications of the proposed configurations. The capital (CAPEX) and operation and maintenance (O&M) costs of the system components are presented in Table 5.

Table 5. *CAPEX and O&M Costs for each unit*

Unit	CAPEX Cost	O&M Costs
MGO	-	728.5 ($/ton)
ORC unit	550,000 $	1.5% of CAPEX / year
Li-ion battery (per module)	54,056 $ [45]	-
Cold ironing receiver	100,000 $ [16]	1000 ($/year) [16]
Generator cost	500 ($/kW) [46]	0.030 ($/h) [46]
Grid electricity (Cold ironing)	-	0.124 ($/kWh) [47]
Grid-PV electricity (Cold ironing)	-	0.147 ($/kWh) [47]

The levelized cost of energy (LCOE), commonly used in the literature to assess the economic viability of energy generation technologies [48-50], is calculated, as shown in Equation 11, using the data in Table 5.

draft copy

$$LCOE = \frac{C_0 + \sum_{y=1}^{N} \frac{C_y}{(1+r)^y}}{\sum_{y=1}^{N} \frac{E_y}{(1+r)^y}} \quad (11)$$

Where C_0 represents the CAPEX for each case, and C_y includes annual O&M and fuel costs. The term N is the system lifetime (years), y is the year index, and E_y considers annual energy demand for each operation mode, including port operations. For clarity and computational convenience, the discount factor (DF) is calculated separately using Equation 12 and subsequently applied in the LCOE calculation [48].

$$DF = \frac{1}{(1+r)^y} \quad (12)$$

In the DF calculation, the ship's lifetime is assumed to be 20 years, in line with values reported in the literature [51-53]. The interest rate (r) is set at 8%. Additionally, the fuel-based unit electricity cost, c_{ele}, is calculated as the ratio of total fuel cost to total electrical energy demand, as given in Equation 13 [54].

$$c_{ele} = \frac{\sum_{i=1}(m_{fuel,i} \times c_{fuel})}{\sum_{i=1}(P_{demand,i} \times \Delta t_i)} \quad (13)$$

Where, m_{fuel} represents the consumed fuel in kg per operation mode, c_{fuel} is the fuel price ($/kg), P_{demand} is the power demand for each operation (kW), and Δt is the operation time (h).

3. Results and Discussion

The power output generated by the ORC unit has been calculated for varying exhaust mass flow rates and temperatures for each refrigerant listed in Table 2. These data, which correspond to the main engine loads outlined in Figure 1, are illustrated in Figure 4.

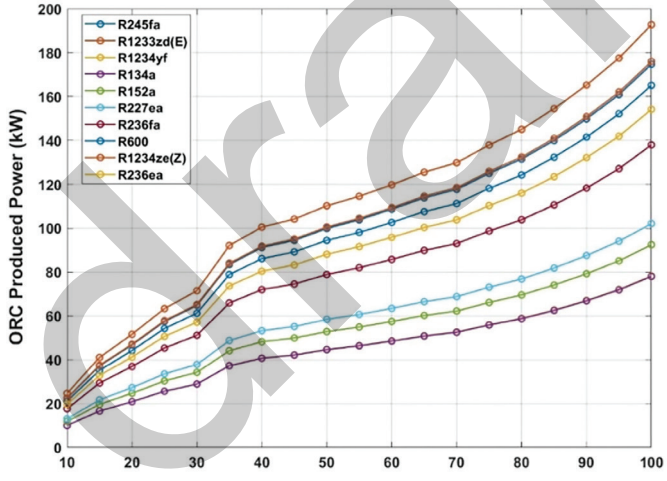

Figure 4. *Variation of net ORC power output with engine load for different working fluids*

ORC: Organic Rankine Cycle

The local power peaks observed at around 35% arise from the non-linear dependence of exhaust gas temperature on engine load, which governs the thermal input available to the ORC system. As shown in Figure 4, R134a consistently yields the lowest power output, reaching 44.59 kW at 50% load and 9.99 kW at 10% load. In contrast, R1233zd(E) exhibits the highest performance, producing 137.92 kW at 50% load and up to 192.74 kW at full load, while decreasing to 24.69 kW at 10% load; this efficiency is consistent with the literature and falls within the commonly reported range for marine ORC systems with power outputs below 200 kW. For the following calculations, the best-performing fluid, R1233zd(E), is selected. The values from Table 3, along with the associated temperature and mass flow rate determined by the load, are used in the ORC cycle with R1233zd(E).

For cruising operations, the power output is 154.44 kW, resulting in 1,236 kWh per duty cycle. Combining Cruise 1 and Cruise 2 yields a total of 2,471 kWh. DP maintains a load of 85%, matching the power output during cruising phases and keeping total energy production at 2,471 kWh. Standby operation has the lowest power output (119.799 kW) but maximizes energy production (22,043 kWh) over a longer duration. The ORC system is inactive during port operations, contributing no power or energy. Unlike conventional oceangoing vessels, PSVs spend a significant portion of their operational life in standby and DP modes, where the availability and duration of waste heat differ substantially. The finding that standby operation contributes the largest share of recoverable energy suggests that system sizing and control strategies should prioritize long-duration, moderate-load conditions rather than peak-load optimization. In addition, the relatively modest ORC power output (≈120-155 kW across most modes) compared to onboard demand indicates that ORC systems are best deployed as auxiliary load-reduction technologies rather than primary power sources.

In Cruise 1 and DP modes, Cases 1 and 3 achieve identical fuel savings, whereas Case 2 shows no improvement over the Base Case because ORC output is prioritized for battery charging. During standby operation, fuel consumption decreased from 22,959.3 kg in the Base Case to 19,913 kg in Case 2; the lowest value was observed in Cases 1 and 3 (18,355.2 kg). Once the batteries in Case 2 are fully charged, fuel consumption in Cruise 2 becomes identical across all ORC-based cases. In port mode, fuel consumption is eliminated in Case 2 via battery supply and in Case 3 via cold ironing, whereas Case 1 relies entirely on generators, resulting in fuel consumption identical to that in the Base Case.

draft copy

Following this, considering fuel consumption and additional scenarios in port, the $CO_{2\text{-eq}}$ Emissions per mode for each case in the PSV's one duty cycle are shown in Figure 5.

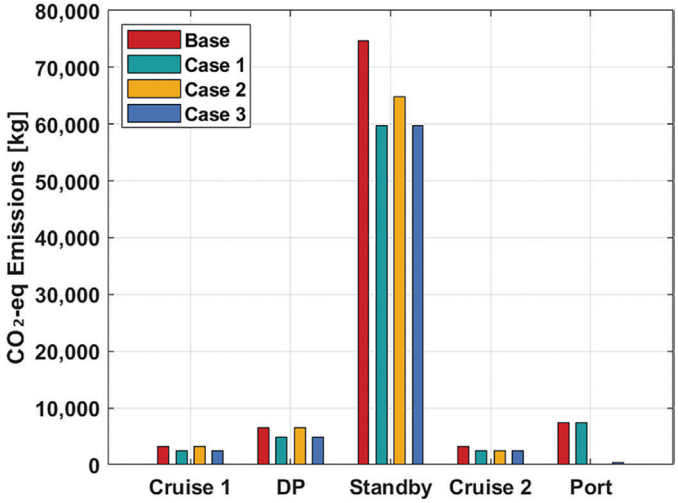

Figure 5. *$CO_{2\text{-eq}}$ emissions per operation mode for each case*

$CO_{2\text{-eq}}$ emission profiles follow the previously discussed fuel consumption trends. ORC-based configurations (Cases 1-3) consistently outperform the base case due to reduced generator loading, yielding moderate yet systematic emission reductions. The most pronounced differences occur during port operations, where the choice of energy supply, rather than fuel consumption alone, determines emissions outcomes. While the base case and Case 1 exhibit the highest $CO_{2\text{-eq}}$ emissions, Case 2 achieves zero emissions by fully supplying port demand via battery power. In contrast, Case 3 employs PV-based grid electricity supply through cold ironing, resulting in a small but near-zero $CO_{2\text{-eq}}$ footprint.

In Case 2, the battery state of charge (SOC) varies continuously across operating modes. Starting from a fully depleted state, SOC increases to 11.3% by the end of Cruise 1 and to 33.8% during DP. During standby operation, the batteries reach 100% SOC; therefore, the subsequent Cruise 2 operation has no impact on battery SOC. The fully charged batteries are then used to supply the entire electrical demand in the port. Since the battery capacity slightly exceeds the energy requirement in the port, a residual SOC of 1.4% remains at the end of port operation. Figure 6 presents the detailed evolution of SOC in Case 2. It highlights the battery's charging and discharging behavior across different operating modes.

Total CO_2 emissions and fuel consumption by case, for one full cycle operation (cruise-DP-standby-port), are represented in Figure 7.

As expected, the base case scenario, which does not incorporate a WHR system, demonstrates the highest levels of consumption and, consequently, emissions. The total emissions recorded are 95,166.7 kg $CO_{2\text{-eq}}$, with a fuel consumption of 29,236.2 kg. Cases 1 and 2 have almost identical fuel consumption and emission results, with values of 23,594.1 kg and 76,801 kg $CO_{2\text{-eq}}$ for Case 1, and 23,646.4 kg and 76,971.5 kg $CO_{2\text{-eq}}$ for Case 2, respectively. The distinction between these two scenarios is not associated with their environmental impact; rather, it stems from considerations of cost and practicality. In addition, Case 3 yields the most favorable outcomes, with 69,723.3 kg $CO_{2\text{-eq}}$ emissions and 21,310.2 kg of fuel consumption.

Following this, emissions from port operations are examined in greater detail for all defined cases. In the base case, where electricity is supplied by MGO-based generators, the $CO_{2\text{-eq}}$ emissions for a single port operation cycle amount to 7,434.37 kg. A similar emission level is obtained for Case 1 (ORC), since port electricity demand is still fully supplied by the MGO generators. For Case 2, port operations are

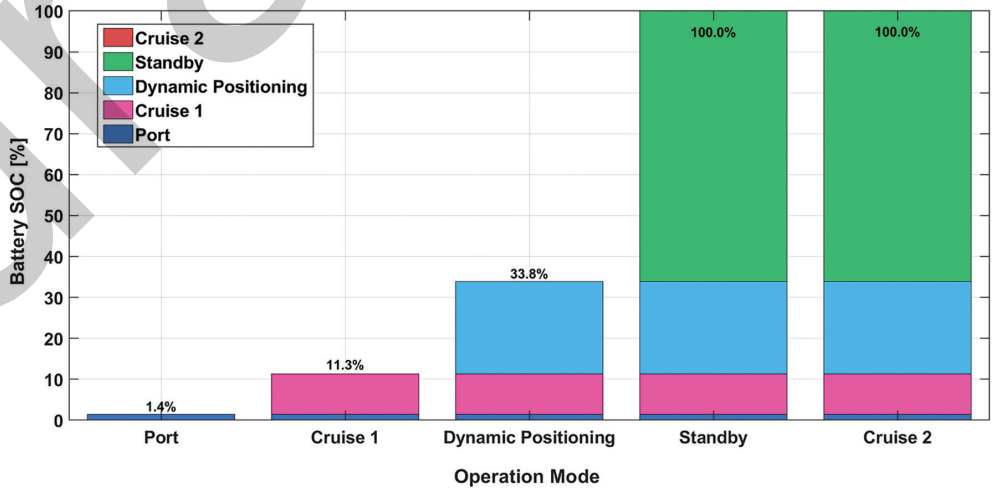

Figure 6. *Battery SOC level per operation mode for Case 2*

draft copy

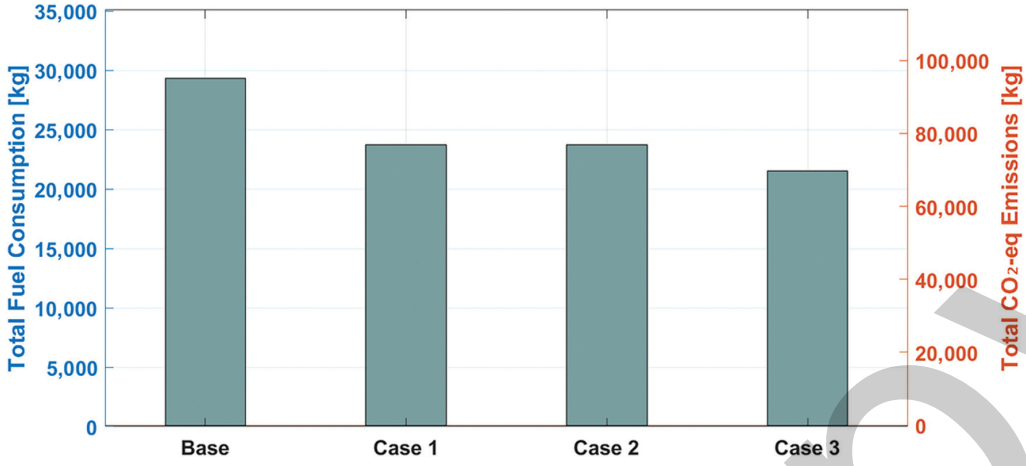

Figure 7. *Total CO_2 emissions and fuel consumption by cases for a full duty operation cycle*

entirely powered by batteries; therefore, operational $CO_{2\text{-eq}}$ emissions are zero. For Case 3, cold ironing significantly reduces port emissions, resulting in emissions of 5,162.4 kg when electricity is supplied from the grid, while PV-based cold ironing further lowers emissions to 356.6 kg. These results clearly demonstrate the strong potential for shore power to mitigate emissions, particularly when coupled with renewable energy sources. Following this, the $CO_{2\text{-eq}}$ emissions and electricity costs for annual port operations are shown in Figure 8.

In Figure 8, the onboard diesel generators using MGO fuel result in the highest $CO_{2\text{-eq}}$ emissions of 223,031 kg at a cost of $49,915 per year. Cold ironing using grid-PV and grid-mix electricity yields comparable costs. The annual electricity cost for PV ($47,628) is higher than that for the grid ($40,176). However, there is a notable difference in emissions: grid electricity generates 154,872 kg, compared with 10,692 kg for the PV system. This is primarily due to the significantly higher $CO_{2\text{-eq}}$ emission factor of grid electricity, reflecting its reliance on fossil-fuel-based power generation.

The economic feasibility of the proposed configurations is assessed using the levelized cost of electricity (LCOE). The base case yields an LCOE of 0.1621 $/kWh. Case 1 and Case 3 exhibit similar economic performance, with LCOE values of 0.1481 $/kWh and 0.1502 $/kWh, respectively. The highest LCOE is observed in Case 2, reaching 0.2098 $/kWh, primarily due to the high capital cost associated with battery integration. While Case 2 offers operational flexibility and zero-emission port operation, these environmental benefits come at the expense of a substantially higher capital investment, thereby undermining its overall feasibility for offshore PSV applications.

The long-term economic performance of the proposed configurations is assessed using cumulative discounted cash flow to determine the PBP based on LCOE values. Figure 9 illustrates the cumulative cash flow for all cases over the project lifetime.

Case 1 achieves a positive return on investment within 6.27 years, driven by reduced annual fuel consumption. Similarly, Case 3 exhibits comparable economic performance for both grid-based and PV-based cold ironing. The additional

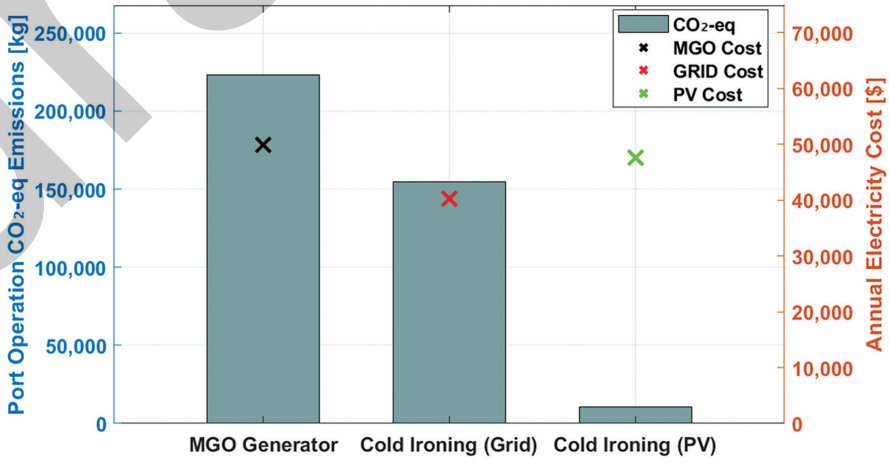

Figure 8. *$CO_{2\text{-eq}}$ emissions (kg) and electricity costs for annual port operation*

draft copy

receiver investment increases the initial CAPEX, resulting in longer PBPs: approximately 7.08 years for the grid-based cold ironing and 7.7043 years for the PV-based configuration. In contrast, Case 2 demonstrates significantly different economic behavior. Although fuel savings similar to Case 1 are achieved, the substantially higher initial investment for battery integration cannot be recovered by operational cost reductions over the vessel's lifetime. Consequently, Case 2 does not reach breakeven within the system lifetime, yielding no discounted PBP, as illustrated in Figure 9b.

To assess the influence of key economic parameters, including MGO fuel price, ORC Capex, interest rate, and carbon tax, a sensitivity analysis is conducted. The selected carbon tax levels of 50, 100, 200, and 300 \$/t CO_2 are intended to reflect both current and prospective regulatory conditions. A carbon tax level of approximately \$50/t CO_2 represents values that are commonly discussed and partially implemented in several European countries. However, it is widely recognized that carbon prices at this level remain insufficient to meet long-term emission reduction targets [55].

In addition, while carbon pricing has been discussed within the IMO framework, including proposals referring to levels around \$100/t CO_2, a comprehensive and binding carbon tax covering total CO_2 emissions has not yet been implemented for the maritime sector [4]. Meanwhile, several countries have announced national-level policies to progressively increase carbon prices for shipping activities, reaching approximately \$130/t CO_2 [56]. Moreover, ongoing alignment efforts between Turkiye and the EU on emissions trading mechanisms, together with current EU carbon allowance prices of around €82/t CO_2 and the upward trend in carbon credit markets, are considered in selecting carbon pricing scenarios. Since a comprehensive carbon pricing scheme is not yet in force for the maritime sector, carbon tax scenarios are excluded from the base case and instead evaluated parametrically at 50, 100, 200, and 300 \$/t CO_2, based on fuel consumption across the vessel's entire operational profile.

Table 6 presents a sensitivity analysis of the discounted PBP for Cases 1 and 3 (PV), illustrating how variations in these parameters affect the PBP performance of each configuration.

The sensitivity analysis (Table 6) reveals that MGO fuel price and carbon taxation are the primary drivers of economic feasibility. Increasing MGO prices and carbon taxes shorten the PBP in Cases 1 and 3, with carbon taxation showing a pronounced non-linear effect at higher levels. Specifically, a \$300/ton CO_2 tax reduces the PBP of Case 1 by 64.4% (to 2.23 years) and Case 3 by 72.5% (to 2.12 years). Conversely, ORC CAPEX shows a direct correlation with PBP, while interest rate variations (6-12%) exhibit a moderate influence. These results underscore that while

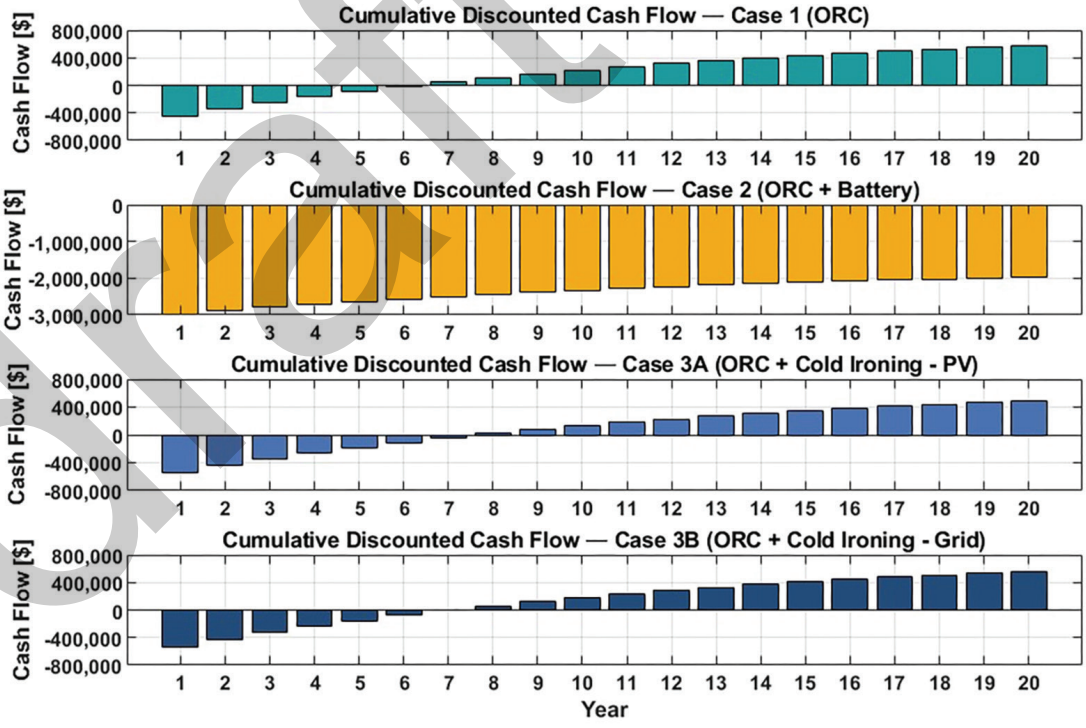

Figure 9. *Cash flow (\$) over the years, representing the discounted PBP for* ***(a)*** *Case 1,* ***(b)*** *Case 2,* ***(c)*** *Case 3-ORC and cold ironing in port with PV,* ***(d)*** *Case 3-ORC and cold ironing in port with grid electricity*

draft copy

Table 6. *Sensitivity analysis of discounted PBP for Case 1 and Case 3 (PV)*

Parameter	Variation	Case 1 PBP (Years)	Case 3 (PV) PBP (Years)	Change in PBP (%)
Baseline scenario	0%	6.27	7.70	-
MGO fuel price	+20% ($874.2/t)	4.92	5.50	-21.5%/-28.6%
MGO fuel price	-20% ($582.8/t)	8.67	13.15	+38.3%/+70.8%
ORC CAPEX	+20% ($660k)	8.15	9.82	+30.0%/+27.5%
ORC CAPEX	-20% ($440k)	4.67	5.93	-25.5%/-23.0%
Interest rate (r)	6%	5.81	7.01	-7.3%/-9.0%
Interest rate (r)	10%	6.82	8.59	+8.8%/+11.6%
Interest rate (r)	12%	7.54	9.80	+20.3%/+27.3%
Carbon tax	$50/ton CO_2	4.80	5.34	-23.4%/-30.6%
Carbon tax	$100/ton CO_2	3.89	4.09	-37.9%/-46.9%
Carbon tax	$200/ton CO_2	2.83	2.80	-54.9%/-63.6%
Carbon tax	$300/ton CO_2	2.23	2.12	-64.4%/-72.5%

fuel-efficient cases lose their advantage if MGO prices drop, carbon pricing significantly offsets the investment costs and aligns with stringent emissions regulations.

The sensitivity analysis further indicates that carbon pricing is a decisive enabler of technology adoption. At carbon tax levels of $100-300/t$CO_2$, PBPs drop dramatically to approximately 2-4 years, transforming ORC-based systems from marginal investments into economically attractive solutions. This finding supports ongoing discussions within international and regional regulatory frameworks, suggesting that carbon pricing mechanisms can effectively bridge the gap between environmental performance and economic feasibility. Moreover, the strong dependence of the benefits of cold ironing on grid emission factors highlights the need for policy coordination between the maritime and energy sectors, ensuring that shore power is increasingly supplied with low-carbon electricity.

The study presents a techno-economic and environmental assessment of ORC-based WHR and cold ironing onboard an offshore PSV, offering insights into decarbonization in the maritime sector. However, some limitations are worth noting: the ORC model assumes steady-state operation under fixed conditions and uses optimistic efficiency parameters, which may lead to overestimation of actual system performance. The battery system is sized to meet the full port energy demand based on simplified assumptions that neglect charge/discharge efficiency losses, depth-of-discharge constraints, and capacity degradation. These assumptions may affect the accuracy of the sizing and the economic outcomes. The analysis focuses on a single vessel, limiting its applicability to other PSV types or to fleet assessments. Nonetheless, the findings lay a solid foundation for understanding the performance of different WHR approaches and carbon-emissions strategies, and, through sensitivity analysis, highlight their economic importance.

4. Conclusion

A thermodynamic ORC model was developed in MATLAB using the CoolProp library, incorporating vessel operating modes and corresponding power demands. After evaluating multiple working fluids, R1233zd(E) exhibited the best performance across all loads, delivering 192.74 kW at full load and an electrical efficiency of 13.77% at 85% load. The selected ORC configuration was subsequently assessed under four operating modes (Cruise, DP, Standby, and Port) and four scenarios (Base Case and Cases 1-3) through environmental ($CO_{2\text{-eq}}$ emissions) and economic (LCOE and PBP) analyses.

- Base Case: The base case (a scenario without an ORC system) exhibited the highest fuel consumption and emissions. Total fuel consumption was 29,236.2 kg, and $CO_{2\text{-eq}}$ emissions amounted to 95,166.7 kg. The LCOE was $0.1621/kWh.

- Case 1: An ORC system was included in addition to the Base Case, and the generated power was used directly to meet the vessel's needs. Total fuel consumption was 23,594.1, and the $CO_{2\text{-eq}}$ emissions were 76,801.3 kg. The obtained LCOE value was $0.1481/kWh.

- Case 2: Primarily feeding the batteries, the ORC system resulted in total fuel consumption of 23,646.4 kg and $CO_{2\text{-eq}}$ emissions of 76,971.5 kg, with a LCOE value of $0.2098/kWh.

- Case 3: Employing cold ironing (PV) during port operation, consumed 21,310.2 kg of fuel, produced 69,723.3 kg of $CO_{2\text{-eq}}$ emissions, and had an LCOE of $ 0.1502/kWh.

draft copy

Considering fuel-related electricity costs, the base configuration has a cost of $0.1517/kWh, while the ORC-integrated configuration achieves a lower cost of $0.1224/kWh. The discounted PBP analysis revealed that Case 1 had the shortest PBP, below 6.27 years, while Case 3 remained economically attractive, with PBPs of 7.08 years for grid-mix and 7.70 years for grid-PV-based cold ironing. In contrast, Case 2 did not reach break-even within the system lifetime, indicating limited economic feasibility under the assumed cost structure. Nevertheless, Case 2 highlights the trade-off between decarbonization objectives and economic performance when battery storage is integrated into ORC-based ship energy systems. The sensitivity analysis further indicates that the discounted PBP is primarily influenced by fuel-related parameters. Variations in MGO fuel prices and carbon taxes have the greatest influence on economic performance, with increases in both significantly reducing the PBP for Cases 1 and 3. In contrast, alterations in ORC capital cost have a moderate but noticeable impact, while variations in the interest rate show the least sensitivity among the parameters considered.

From an integration perspective, the comparison of Cases 1-3 demonstrates that system simplicity and utilization rates are critical to feasibility. Direct ORC integration (Case 1) achieves the most balanced outcome due to continuous utilization and minimal additional complexity. In contrast, battery coupling (Case 2), while operationally flexible, introduces significant capital costs without a proportional economic return, indicating that battery sizing must be carefully optimized or justified by stricter zero-emission requirements. The strong performance of the ORC-cold ironing configuration (Case 3) further suggests that hybridization between onboard WHR and shore-based solutions represents a practical pathway, especially for vessels with long port stays. This has direct implications for retrofit strategies, where modular ORC units, combined with shore power compatibility, can deliver incremental yet meaningful efficiency gains.

Overall, the results demonstrate that ORC-based WHR, when combined with appropriate energy management strategies such as cold ironing, can significantly enhance both the environmental and economic performance of offshore PSVs. The outcomes of this study align closely with emerging maritime decarbonization policies, particularly those targeting both operational efficiency (e.g., EEXI, CII) and port emissions (e.g., FuelEU Maritime, green port mandates). The observed 26.7% reduction in $CO_{2\text{-eq}}$ emissions for the ORC-cold ironing configuration demonstrates that compliance with increasingly stringent carbon intensity targets can be achieved through combined onboard and port-based measures, rather than relying on a single technology. Importantly, the results show that cold ironing provides the largest marginal emission reduction during port operations, reinforcing regulatory trends that mandate shore power use in major ports. The direct ORC integration and ORC-cold ironing configurations identified in this work represent economically viable implementation pathways for offshore PSVs, particularly under scenarios involving rising fuel prices and carbon taxation. Port authorities may use these results to support investments in shore power infrastructure, while policymakers can benefit from the reported emission reduction benchmarks when developing relevant regulatory frameworks.

Building on the findings of this study, several directions for future research can be identified. First, the present work relies on a steady-state modeling approach; therefore, dynamic, time-resolved simulations incorporating real voyage data would improve the accuracy of performance and economic assessments, particularly for vessels with highly variable load profiles. Second, further research is needed for advanced control strategies for ORC systems, including adaptive operation under fluctuating engine loads and integration with ship energy management systems. In addition, future studies should explore hybrid configurations with optimized battery sizing, alternative storage technologies, or second-life batteries to improve cost-effectiveness. Another promising direction involves the integration of ORC systems with emerging technologies such as carbon capture, alternative fuels (e.g., methanol, ammonia), or supercritical CO_2 cycles, which may significantly enhance overall system efficiency.

Footnotes

Authorship Contributions

Concept design: O. Konur, Data Collection or Processing: C. Çelebi, O. Konur, and S. A. Korkmaz, Analysis or Interpretation: C. Çelebi, O. Konur, and S. A. Korkmaz, Literature Review: C. Çelebi, and O. Konur, Writing Reviewing and Editing: C. Çelebi, O. Konur, and S. A. Korkmaz.

Declaration on the Use of Artificial Intelligence (AI): Artificial intelligence has been used to assist with "text editing".

Funding: The authors did not receive any financial support for the research, authorship, and/or publication of this article.

References

[1] L. Bilgili, and A. I. Ölçer, "IMO 2023 strategy-Where are we and what's next?," *Marine Policy*, vol. 160, 105953, Feb 2024.

[2] E. Czermański, et al. "Implementation of the energy efficiency existing ship index: an important but costly step towards ocean protection," *Marine Policy*, vol. 145, 105259, Nov 2022.

draft copy

[3] S.-S. Lee, "Analysis of the effects of EEDI and EEXI implementation on CO2 emissions reduction in ships," *Ocean Engineering*, vol. 295, 116877, Mar 2024.

[4] "IMO. (2025). Draft amendments to MARPOL Annex VI Regulations for the prevention of air pollution from ships. Circular Letter No. 5005".

[5] I. Maritime Organization, "IMO. (2022). 2022 guidelines for the development of a ship energy efficiency management plan (SEEMP). Annex 8 Resolution MEPC.346(78)".

[6] O. Konur, C. O. Colpan, and O. Y. Saatcioglu, "A comprehensive review on organic Rankine cycle systems used as waste heat recovery technologies for marine applications," *Energy Sources, Part A: Recovery, Utilization, and Environmental Effects*, vol. 44, pp. 4083-4122, Jun 2022.

[7] T. P. V. Zis, "Prospects of cold ironing as an emissions reduction option," *Transportation Research Part A: Policy and Practice,* vol. 119, pp. 82-95, Jan 2019.

[8] S. Kose, and D. M. Sekban, "Emphasizing the importance of using cold-ironing technology by determining the share of hotelling emission value within the total emission," *Transportation Safety and Environment*, vol. 4, tdac010, Jun 2022.

[9] K. P. Peddi, S. Ricci, and L. Rizzetto, "Reduction potential of gaseous emissions in European ports using cold ironing," *Applied Sciences*, vol. 14, 6837, Aug 2024.

[10] M. Canepa, F. Ballini, D. Dalaklis, G. Frugone, and D. Sciutto, "Cold ironing: socio-economic analysis in the port of Genoa," *Logistics*, vol. 7, p. 28, May 2023.

[11] J. Qiu, Y. Tao, S. Lai, and J. Zhao, "pricing strategy of cold ironing services for all-electric ships based on carbon integrated electricity price," *IEEE Transactions on Sustainable Energy,* vol. 13, pp. 1553-1565, Jul 2022.

[12] M. Gianni, A. Pietra, A. Coraddu, and R. Taccani, "Impact of SOFC power generation plant on carbon intensity index (CII) calculation for cruise ships," *Journal of Marine Science and Engineering,* vol. 10, p. 1478, Oct 2022.

[13] S.-T. Le, "Research on drivers and barriers to the implementation of cold ironing technology in zero emissions port," *Environmental Health Insights,* vol. 18, Jan 2024.

[14] R. Glavinović, M. Krčum, L. Vukić, and I. Karin, "Cold ironing implementation overview in European ports—case study—Croatian ports," *Sustainability*, vol. 15, p. 8472, May 2023.

[15] D. Tang, et al. "Assessing the potential for energy efficiency improvement through cold ironing: a Monte Carlo analysis with real port data," *Journal of Marine Science and Engineering,* vol. 11, 1780, Sep 2023.

[16] N. N. Abu Bakar, T. Uyanik, Y. Arslanoglu, J. C. Vasquez, and J. M. Guerrero, "Two-stage energy management framework of the cold ironing cooperative with renewable energy for ferry," *Energy Conversion and Management,* vol. 311, 118518, Jul 2024.

[17] O. Yuksel, M. Bayraktar, and A. Seyhan, "Environmental and economic analysis of cold ironing using renewable hybrid systems," *Clean Technologies and Environmental Policy,* vol. 27, pp. 3489-3517, Aug 2025.

[18] O. Yuksel, and B. Koseoglu, "Numerical simulation of the hybrid ship power distribution system and an analysis of its emission reduction potential," *Ships and Offshore Structures*, vol. 18, pp. 78-94, Jan 2023.

[19] T. Miller, I. Durlik, E. Kostecka, P. Kozlovska, A. Jakubowski, and A. Łobodzińska, "Waste heat utilization in marine energy systems for enhanced efficiency," *Energies (Basel)*, vol. 17, 5653, Nov 2024.

[20] A. Pesyridis, M. S. Asif, S. Mehranfar, A. Mahmoudzadeh Andwari, A. Gharehghani, and T. Megaritis, "Design of the organic rankine cycle for high-efficiency diesel engines in marine applications," *Energies (Basel)*, vol. 16, 4374, May 2023.

[21] L. Lyu, A. Kan, W. Chen, Y. Zhang, and B. Fu, "Energy, exergy and environmental analysis of ORC waste heat recovery from container ship exhaust gases based on voyage cycle," *Journal of Marine Science and Engineering,* vol. 11, 2029, Oct 2023.

[22] C. Ezgi, and H. Kepekci, "Thermodynamic analysis of marine diesel engine exhaust heat-driven organic and inorganic rankine cycle onboard ships," *Applied Sciences*, vol. 14, 7300, Aug 2024.

[23] O. Konur, O. Yuksel, S. Aykut Korkmaz, C. Ozgur Colpan, O. Y. Saatcioglu, and B. Koseoglu, "Operation-dependent exergetic sustainability assessment and environmental analysis on a large tanker ship utilizing organic rankine cycle system," *Energy*, vol. 262, 125477, Jan 2023.

[24] W. Chen, S. Xue, L. Lyu, W. Luo, and W. Yu, "Energy saving analysis of a marine main engine during the whole voyage utilizing an organic rankine cycle system to recover waste heat," *Journal of Marine Science and Engineering,* vol. 11, 103, Jan 2023.

[25] T. Ouyang, Y. Huang, X. Tuo, H. Zhou, and C. Mo, "Comprehensive performance analysis and optimization of an ORC-HDH system for power and freshwater production driven by marine exhaust gas," *Desalination*, vol. 592, 118166, Dec 2024.

[26] S. Yao, X. Yan, M. Xia, C. Wang, and S. Wang, "Thermodynamic and economic analysis, optimization of SOFC/GT/SCO2/ORC hybrid power systems for methanol reforming-powered ships with carbon capture," *Case Studies in Thermal Engineering*, vol. 67, 105840, Mar 2025.

[27] P. A. Duong, B. Ryu, C. Kim, J. Lee, and H. Kang, "Energy and exergy analysis of an ammonia fuel cell integrated system for marine vessels," *Energies (Basel)*, vol. 15, 3331, May 2022.

[28] Z. Tian, Y. Zhou, P. Bolat, Y. Zhang, and W. Gao, "Responding to low-carbon shipping via a novel BOG-ORC-CCS system onboard LNG carrier: 4E analyses and optimization," *Journal of Cleaner Production,* vol. 478, 143959, Nov 2024.

[29] X. Yan, J. Sun, and S. Yao, "Design, thermodynamic and economic analysis, and optimization of a carbon capture integrated energy system for LNG-powered ships," *Applied Thermal Engineering,* vol. 267, 125728, May 2025.

[30] F. Reale, R. Calabria, and P. Massoli, "Performance analysis of WHR systems for marine applications based on sCO_2 gas turbine and ORC," *Energies (Basel)*, vol. 16, 4320, May 2023.

[31] S. Zhao, K. Pazouki, and R. Norman, "Performance evaluation of combined wind-assisted propulsion and organic rankine cycle systems in ships," *Journal of Marine Science and Engineering,* vol. 13, 1287, Jun 2025.

[32] G. Kosmadakis, and P. Neofytou, "Reversible high-temperature heat pump/ORC for waste heat recovery in various ships: a techno-economic assessment," *Energy*, vol. 256, 124634, Oct 2022.

[33] O. Konur, O. Yuksel, S. A. Korkmaz, C. O. Colpan, O. Y. Saatcioglu, and I. Muslu, "Thermal design and analysis of an organic rankine cycle system utilizing the main engine and cargo oil pump turbine

draft copy

based waste heats in a large tanker ship," *Journal of Cleaner Production,* vol. 368, 133230, Sep 2022.

[34] "Scania Engines, (2012). Technical Data DI12 62M. EM 11420: - Engineering Manual. Rev 11.6.201. Nogva Motorfabrikk AS."

[35] "Everllence, (2025). CEAS engine calculations." Accessed: Feb. 08, 2026. [Online]. Available: https://www.everllence.com/marine/products/planning-tools-and-downloads/ceas-engine-calculations

[36] M. G. Çıvgın, and C. Deniz, "Environmental-based working fluid selection for organic rankine cycle for waste heat recovery in marine diesel engines," *Journal of Marine Science and Application*, Apr 2026.

[37] L. Lyu, W. Chen, A. Kan, Y. Zhang, S. Xue, and J. Zeng, "Investigation of a dual-loop ORC for the waste heat recovery of a marine main engine," *Energies (Basel)*, vol. 15, 8365, Nov 2022.

[38] S. Lebedevas, and T. Čepaitis, "Complex use of the main marine diesel engine high- and low-temperature waste heat in the organic rankine cycle," *Journal of Marine Science and Engineering,* vol. 12, 521, Mar 2024.

[39] Greenhouse Gas Protocol, "IPCC Global Warming Potential Values. Version No. 2.0, Date. August 7, 2024, updated with AR6 values." [Online]. Available: https://ghgprotocol.org/sites/default/files/2024-08/Global-Warming-Potential-Values %28August 2024%29.pdf

[40] EPA, "Technology Transitions GWP Reference Table." [Online]. Available: https://www.epa.gov/climate-hfcs-reduction/technology-transitions-gwp-reference-table

[41] I. Maritime Organization, "International Maritime Organization (IMO), "Resolution MEPC.391(81): Regulatory framework for MARPOL Annex VI emission amendments," MEPC 81, 2024. [Online]. Available: https://wwwcdn.imo.org/localresources/en/KnowledgeCentre/IndexofIMOResolutions/MEPCDocuments/MEPC.391(81).pdf. Accessed: Aug. 04, 2025."

[42] IPCC, (2013). Climate change 2013: the physical science basis. Contribution of Working Group I to the Fifth Assessment Report of the Intergovernmental Panel on Climate Change. Cambridge University Press.

[43] "T.C. ETKB, (2025). Türkiye elektrik üretimi ve elektrik tüketim noktası emisyon faktörleri. Accessed: Jul 31, 2025 from https://enerji.gov.tr/evced-cevre-ve-iklim-elektrik-uretim-tuketim-emisyon-faktorleri."

[44] "IEA, life cycle upstream emissions factors." Accessed: Feb 08, 2026. [Online]. Available: https://www.iea.org/data-and-statistics/data-product/life-cycle-upstream-emissions-factors-2024-2#life-cycle-upstream-emission-factors

[45] "SHANGHAI Elecnova." Accessed: Dec 21, 2025. [Online]. Available: https://elecnova.en.made-in-china.com/

[46] R. Iqbal, Y. Liu, Y. Zeng, Q. Zhang, and M. Zeeshan, "Comparative study based on techno-economics analysis of different shipboard microgrid systems comprising PV/wind/fuel cell/battery/diesel generator with two battery technologies: A step toward green maritime transportation," *Renewable Energy*, vol. 221, 119670, Feb 2024.

[47] "EPDK | Enerji Piyasası Düzenleme Kurumu" Accessed: Feb 08, 2026. [Online]. Available: https://www.epdk.gov.tr/Detay/Icerik/3-1327/elektrik-faturalarina-esas-tarife-tablolari

[48] C. Guo, W. Sheng, D. G. De Silva, and G. Aggidis, "A review of the levelized cost of wave energy based on a techno-economic model," *Energies (Basel)*, vol. 16, 2144, Feb 2023.

[49] A. Martinez, and G. Iglesias, "Multi-parameter analysis and mapping of the levelised cost of energy from floating offshore wind in the Mediterranean Sea," *Energy Conversion and Management,* vol. 243, 114416, Sep 2021.

[50] A. Ioannou, A. Angus, and F. Brennan, "Parametric CAPEX, OPEX, and LCOE expressions for offshore wind farms based on global deployment parameters," *Energy Sources, Part B: Economics, Planning, and Policy*, vol. 13, pp. 281-290, May 2018.

[51] C. Wang, Y. Ju, and Y. Fu, "Comparative life cycle cost analysis of low pressure fuel gas supply systems for LNG fueled ships," *Energy*, vol. 218, 119541, Mar 2021.

[52] E. O. Olaniyi, and G. Prause, "Investment analysis of waste heat recovery system installations on ships' engines," *Journal of Marine Science and Engineering,* vol. 8, 811, Oct 2020.

[53] F. Mylonopoulos, S. Durgaprasad, A. Coraddu, and H. Polinder, "Lifetime design, operation, and cost analysis for the energy system of a retrofitted cargo vessel with fuel cells and batteries," *International Journal of Hydrogen Energy,* vol. 91, pp. 1262-1273, Nov 2024.

[54] O. Yuksel, O. Konur, M. Pamık, and M. Bayraktar, "The economic and environmental assessment of alternative marine fuels and nuclear energy utilization on a floating power plant," *Environmental Science and Pollution Research*, vol. 31, pp. 49780-49799, Jul 2024.

[55] H. Liu, K. Ju, M. Guo, and T. Mao, "Theory and practice of China's shipping carbon tax under the 'dual carbon' targets," *Frontiers in Marine Science,* vol. 12, Oct 2025.

[56] H. Liu, K. Ju, X. Wei, C. Zhang, and J. Zhou, "Shipowners' responses to carbon tax: speed optimization using AIS data," *Clean Technologies and Environmental Policy,* vol. 27, pp. 7663-7678, Dec 2025.

draft copy